Transparent Aerogels with High Mechanical Strength Composed of Cellulose-silica Cross-linked networks

Qing Zhou, Yong Shen, Sufen Ai, Bin Liu and Yingmin Zhao

Aerospace Institute of Advanced Materials & Processing Technology, CHN

Abstract. We prepared monolithic transparent composite aerogels with high mechanical strength composed of cellulose-silica interpenetrating polymer network (IPN) structures. Cellulose-silica areogels were obtained by dissolving cellulose in silica hydrogels, followed by gelling, aging and drying using supercritical drying. The composite nanonetworks of cellulose-silica areogels were demonstrated with scanning electron microscope (SEM). The density of cellulose-silica aerogels is between 20 and 38 kg/m^3. The surface area of aerogels was between 300 m^2/g to 500 m^2/g.

1 Introduction

Aerogels are highly porous nanostructured materials usually prepared by sol-gel processing followed by supercritical drying whose final stage involved extracting the pore-filling solvent with liquid CO_2 [1-6]. Aerogels which are characterized by large internal surface area and large open pores, are promising candidates for various advanced applications such as thermal insulation, catalysts/catalyst supports, acoustics, and gas filters [7-15].

Currently, the ever worsening problems of fossil energy depletion and global warming have become a major challenge and survival threat to human being, and have thus greatly boosted the research efforts in development of clean alternative energy and emission control of global warming gases. However these effortswould prove insufficient if not accompanied with energy conservation practices. One of the major energy saving practices is thermal insulation, e.g., reducing fuel and electricity usages through better insulating boilers and buildings, respectively. In this situation, aerogels are prospective to be used in the glazing of green buildings because of their near transparency and low thermal conductivity.

Though monolithic transparent aerogels can be facilely prepared from silica aerogels, they suffer from the poor mechanical properties due to the weak chemical bonding among silica nanoparticles. One solution is to fabricate cellulose aerogels [16-19] with interconnected open-porous network structures. However, they’re light-tight, and the preparation process usually involves the utilization of toxic isocyanates. Furthermore， neat aerogels including silica aerogels and cellulose aerogels shrink during production and the shrinkage cracking makes it difficult to form monolithic aerogels. Therefore, a couple of scientific studies have been initiated aiming at the preparation of silica aerogels [20-23].

In this paper, we reported a novel method to fabricate composite cellulose-aerogels with a interpenetrating polymer network (IPN) structure. We used the sol–gel synthesis method toward nanostructured silica, which typically started from tetramethoxysilane (TMOS). The resulting composite aerogels were dried with supercritical CO_2 to give cellulose–silica aerogels which were lightweight, transparent and with good mechanical properties. Ionic liquid was used as a solvent to dissolve native cellulose. The native cellulose was esterifed to make it dissolved well in silica sol solution. The cellulose-silica composite areogels can be used as glazing in energy-saving building.

2 Experimental section

2.1 Preparation

2.1.1 Materials

Tetramethoxysilane (TMOS) were purchased from Sigma-Aldrich. Fibrous native cellulose (Ashless pulp. Advantec, Japan), n-Butyric anhydride, hydrochloric acid (37%), formic acid and ethanol (EtOH) were obtained from Fluka. Ionic liquid (AmimCl) was purchased from Sigma-Aldrich. All reagents were used as received unless otherwise noted.

2.1.2 Cellulose modified

Native cellulose was firstly dissolved in ionic liquid at room temperature with stirring to form a cellulose

solution, and subsequently esterifed by Butyric anhydride with catalysts (ammonia), and three kinds of esterifiable celluloses named P1, P2, P3 which differed in degree of esterification could be obtained.

2.1.3 Wet gel preparation

Cellulose-silica hydrogels were fabricated according to thefollowing procedure:TEOS and EtOH were mixed in a beaker. Then HCl (0.038M) was added and the mixtures were stirred for 1.5h. A solution of esterified cellulose in ethanol was then added to the mixture and stirred for 5min. The wet cellulose-silica hydrogels were obtained after standing for 24h.

2.1.4 Drying method

The cellulose-silica hydrogels were solvent-exchanged with EtOH for 3 times, and then subjected to supercritical carbon dioxide drying. The autoclave is closed and filled with liquid carbon dioxide (CO_2) until the samples are completely immersed in the liquid. The EtOH iscompletely removed after several times washing with pure CO_2.

2.2 Characterization

FTIR measurements were performed on a Perkin-Elmer series 2000 instrument. Sample wafers consisted of 105 mg dry KBr and ca. 1 mg aerogel sample.

^{1}H MAS NMR spectra was obtained on a Bruker DSX-400 spectrometer at 400 MHz.

Densities of the aerogels were calculated by weighting the samples and measuring the volumes.

Scanning electron microscopy (SEM) was conducted on a Hitachi S-4800 microscopy.

The specific surface area of aerogels was measured with the BET method from the nitrogen adsorption in a Coulter SA3100 analyser. The analysis was done for relative vapor pressure of 0.05 to 0.3.

Lard and strain tests of three-point flexural bending method of the composite aerogels were performed on an EZ-test (DDL-100, China) with a deformation rate of 1 mm/min. The aerogels of a size of 80 mm length and a square cross section with an edge length of 20 mm.

3 Results and discussion

Fig. 1 shows the esterification of native cellulose. To distinguish the different degree of esterification, we called the modified cellulose P0, P1, P2 and P3, with P0 representing the original cellulose.

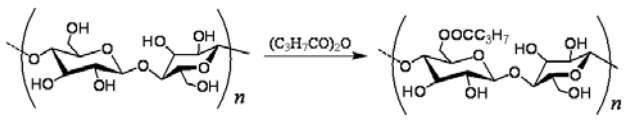

Figure 1. Esterification of native cellulose.

The esterification pruducts of cellulose were characterized by FT-IR and ^{1}H-NMR spectra. Fig. 2 gives the FT-IR spectra of the original cellulose P0 and the esterifiable products P1, P2 and P3, respectively. Compared to the FT-IR spectra of P0, the appearance of absorption located at 1745 cm^{-1} and 1167 cm^{-1} suggests the successful esterification of cellulose. The absorption located at 2968 cm^{-1} and 2870 cm^{-1} can be ascribed to the stretch vibration of methyl group while the absorption located at 2940 cm^{-1} and 1420 cm^{-1} are attributed to methylene group. These results further indicate the successful introduction of alkyl group due to esterification. Moreover, the higher absorbance at 1745 cm^{-1} of P3 compared to that of P2 demonstrates the higher reaction conversion of P3. P1 has the lowest reaction conversion.

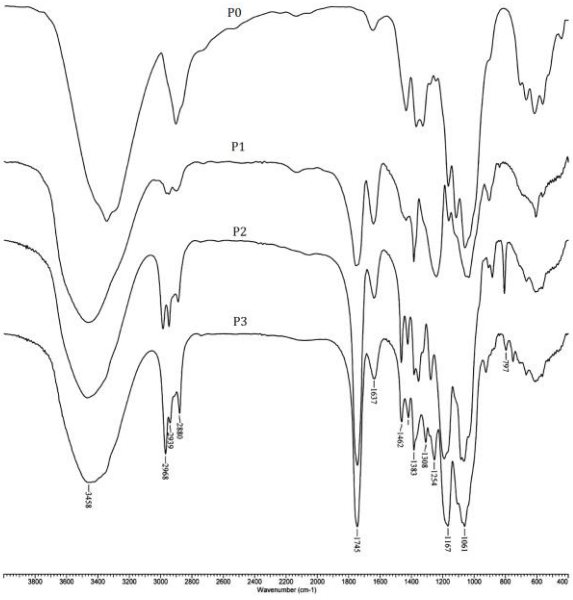

Figure 2. FTIR of native cellulose and esterified cellulose.

The structures of P1, P2 and P3 were further characterized with ^{1}H-NMR spectra. As shown in Fig. 3, the broad peak at 2.2 ppm can be assigned to the resonance of methylene group adjacent to carboxyl group and the broad peak at 1.5 ppm can be attributed to another methylene group. The resonance of methylene group together with that of methyl group at 0.87 ppm demonstrated the successful esterification of cellulose P0. It is worth pointing out that it is difficult to quantitatively calculate the reaction conversion of P1, P2 and P3 due to their poor solubility in DMSO. Sample P3 was chosen to continue the following experiment because of its good solubility in silica solution.

^{13}C-NMR spectrum is another powerful tool in characterization of organic compounds. Fig. 4 gives the ^{13}C-NMR spectrum of P3. The three peaks located at 172.4 ppm, 171.6 ppm, 171.2 ppm can be assigned to the carbon of the ester group. The peak at 35.0, 17.7 ppm and 13.3 ppm can be assigned to the carbon of methylene and methyl group, respectively. The peaks located between 56 ppm and 104 ppm are attributed to the carbon of

glucose unit. P1 and P2 give consistent and similar ^{13}C-NMR spectra with P3. The ^{13}C-NMR spectra further demonstrate the successful esterification of native cellulose.

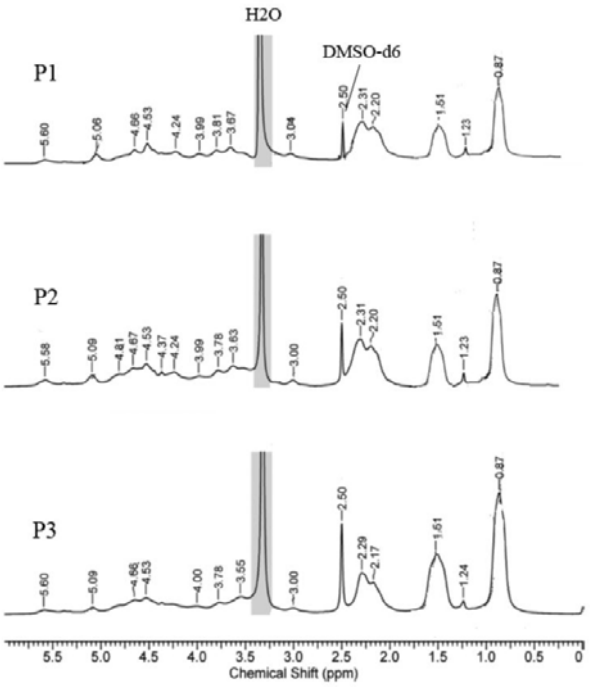

Figure 3. ^{1}H-NMR of P1, P2 and P3.

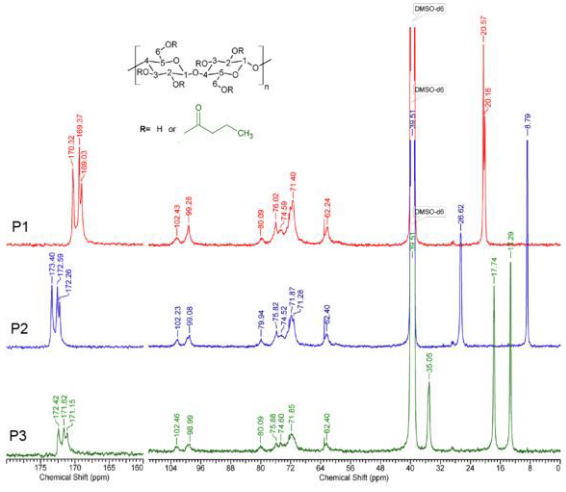

Figure 4. ^{13}C-NMR of P1, P2 and P3.

Scheme 1 explained the mechanism of formic acid catalyzing hydrolysis-condensation of TMOS and silica hydrogels. The whole process took place in ionic liquid. Fig. 5 illustrates the preparation of the cellulose-silica aerogels. The silica hydrogels were firstly formated, then cellulose molecular aggregated around the silica network to form a interpenetrating polymer network (IPN) structure hydrogel, at last the composite hydrogel was supercriticallly dried by liquid CO_2 to obtain silica-cellulose composite aerogels. Fig. 6 shows the pictures of the cellulose-silica hydrogels and aerogels with cellulose concentrations vary from 0.75 wt.% to 10 wt.% respectively. All the hydrogels are transparent without obvious difference, as can be seen from the pictures in Fig. 6. However, the transparency of aerogels decreases as the concentration of cellulose increases. Table 1 summarizes the sample compositions and densities. The sample densities increases from 20 to 38 kg/m^3 as the content of cellulose changes from 0.75 wt.% to 10 wt.% in concentration.

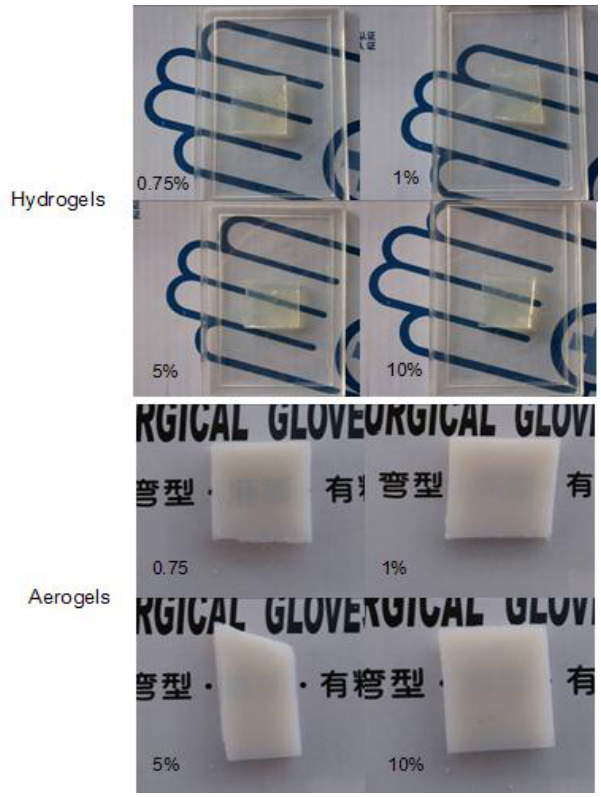

Figure 6. Pictures of cellulose-silica hydrogels and aerogels with different cellulose contents.

Table 1. Densities of aerogels with different cellulose concentrations.

	Cellulose/wt. %	**TEOS/wt.%**	**Density/kg m^{-3}**
IPN1	0.75	8	20
IPN2	1	8	24
IPN3	5	8	29
IPN4	10	8	38

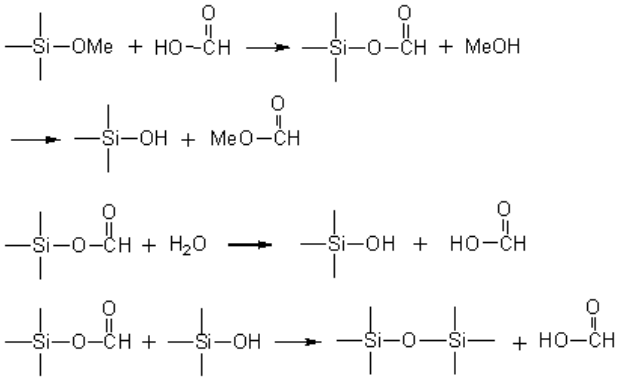

Scheme 1. The mechanism of TMOS hydrolysis-condensation catalyzed by formic acid.

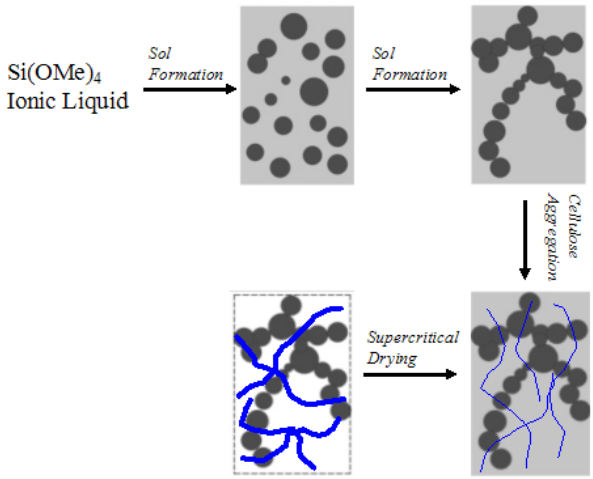

Figure 5. The schematic preparation of Cellulose-silica aerogels.

The microstructures of cellulose-silica aerogels are observed by SEM. These observations indicate that instead of being homogeneous, cellulose particles deposit around silica to form a stronger network. The SEM pictures furthermore demonstrates that the size of composite nanoparticles varies from 50 nm to 1 μm. When the concentration of the cellulose solution is 0.75 wt.%, the diameter of aerogel paricles is about 50 nm. When the concentration of the cellulose solution is 1 wt.%, the diameter of aerogel paricles is about 300 nm; When the concentration of the cellulose solution is 5 wt.%, the diameter of aerogel paricles is about 700 nm; When the concentration of the cellulose solution is 10 wt.%, the diameter of aerogel paricles is about 1 μm. cellulose Those particles are connected by "necks" formed by dissolution and reprecipitation of cellulose during aging. However, the micrographs doesnot show the mesopores which were characterized by the BET method from the nitrogen adsorption.

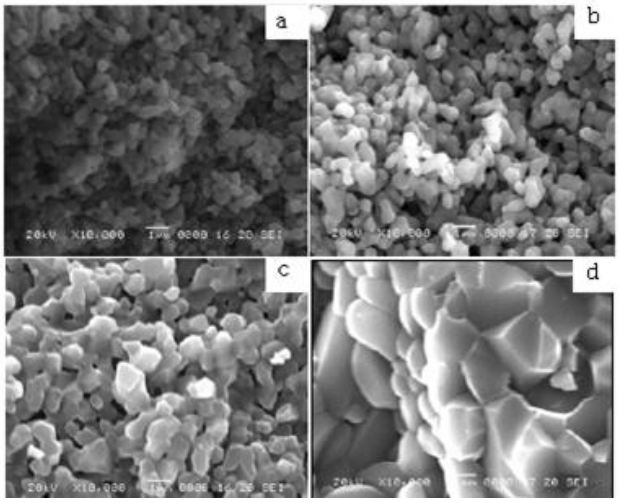

Figure 7. (a) SEM picture of a composite aerogel with 0.75 wt.% cellulose. (b) SEM picture of a composite aerogel with 1 wt.% cellulose. (c) SEM picture a composite aerogel with 5 wt.% cellulose. (d) SEM picture a composite aerogel with 10 wt.% cellulose.

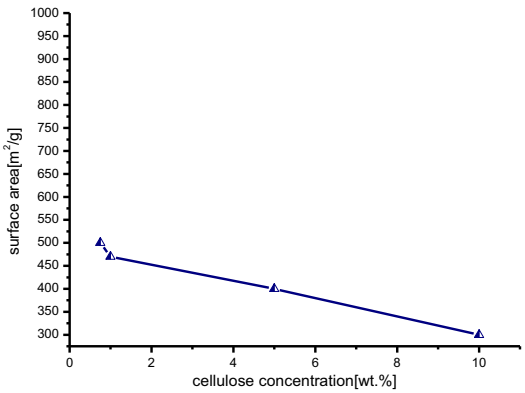

Figure 8. BET-schema for cellulose-silica composite aerogels.

Fig. 8 exhibits the surface area of silica-cellulose composite aerogels produced by different concentration of cellulose solution. The surface area of composite aerogels with 0.75 wt.% cellulose is about 525 m^2/g; The surface area of composite aerogels with 1.00 wt.% cellulose is about 480 m^2/g; The surface area of composite aerogels with 5.00 wt.% cellulose is about 430 m^2/g; the surface area of composite aerogels with 10.00 wt.% cellulose is about 300 m^2/g. The figure of the BET indicates that the surface area of the composite aerogels is inversely proportional to the cellulose concentration, which is consistent with the results from SEM images.

Fig. 9 shows the load-strain curves of four representative composite monoliths on the way to their respective rupture points. The most dramatic improvement of the composite aerogels is in the strength of the new material. It's a test called three point flexural bending method. It takes more than 10 times higher load to break a aerogel monolith with density 0.038 g/cm^3 (12 kg) than to break a aerogel monolith with density 0.020 g/cm^3 (12 kg). The least dense sample is linearly elastic, while the more dense samples behave as nonlinear elastic.

When the density of composite aerogels reaches to 0.038 g/cm^3, the rupture point is about 12 kg that it is strong enough to be carried on.

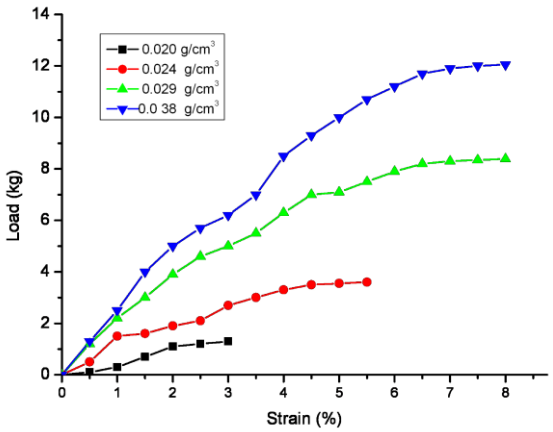

Figure 9. Load-strain curves for the four composites of table 1.

4 Conclusions

High mmechanical strength and flexible cellulose-silica aerogels composed of Cellulose-silica Cross-linked networks were fabricated by sol-gel chemistry using supercritical drying. It's possible to build complex 3D-structures at nanometer range between silica and cellulose. Ionic liquid was used as a solvent to dissolve native cellulose. The native cellulose was esterifed to make it dissolved well in silica sol solution. The molecules of cellulose deposited around the network of silica and reinforced the structure. The cross-linked porous structures can be shown in SEM. Their densities were between 20 and 38 kg/m^3 with concentrations of cellulose between 0.75 wt.% and 10 wt.%. The surface area of aerogels was between 300 m^2/g to 500 m^2/g. When the density of composite aerogels reaches to 0.038 g cm^{-3}, the rupture point is about 12 kg. In this way, it's possible to fabricate glazing used in green building in the future.

Acknowledgments

This work is supported by Chinese state commission of science and technology for national defense industry and it's managed by the aerospace Institute of advanced materials & processing technology, has sponsored this work.

References

1. N. H. Sing, U. Schubert, Angew. Chem. 1998, 110, 22 – 47; Angew. Chem. Int. Ed., **37**, 22 – 45, (1998).
2. A. C. Pierre, G. M. Pajonk, Chem. Rev., **102**, 4243 – 4265, (2002).
3. A. E. Aliev, J. Y. Oh, M. E. Kozlov, A. A. Kuznetsov, S. L. Fang, A. F. Fonseca, R. Ovalle, M. D. Lima, M. H. Haque, Y. N. Gartstein, M. Zhang, A. A. Zakhidov, R. H. Baughman, Science, **323**, 1575 – 1578, (2009).
4. J. L. Mohanan, I. U. Arachchige, S. L. Brock, Science, **307**, 397 – 400, (2005).
5. M. A. Worsley, P. J. Pauzauskie, T. Y. Olson, J. Biener, J. H. Satcher, Jr., T. F. Baumann, J. Am. Chem. Soc., **132**, 14067 – 14069, (2010).
6. I. U. Arachchige, S. L. Brock, J. Am. Chem. Soc., **128**, 7964 – 7971, (2006).
7. J. Fricke, Aerogels, Springer-Verlag, Berlin (1986).
8. R. J. Ayen and P. A. Iacobucci, Reviews in Chemical Engineering **5**, 157(1988).
9. M. Schneider and A. Baiker, Catal. Rev.-Sci. Eng. **37**, 515 (1995).
10. Pajonk, G. M., Catal. Today, **37**, 3(1999).
11. Morris, C. A.; Anderson, M. L.; Stroud, R. M.; Merzbacher, C. I.; Rolison, D. R., Science, **284**, 622(1999).
12. Novak, B. M.; Auerbach, D.; Verrier, C., Chem. Mater., **6**, 282(1994).
13. Jones, S. M. J., Sol-Gel Sci. Tech., **40**, 351(2006).
14. Junga, S. B.; Parka, S. W.; Yanga, J. K.; Park, H. H.; Kimb, H., Thin Solid Films, **580**, 447–448(2004).
15. Tsutsui, T.; Yahiro, M.; Yokogawa, H.; Kawano, K.; Yokoyama, M.; AdV. Mater., **13**, 1149(2001).
16. Fischer F, Rigacci A, Pirard R, Berthon-Fabry S, Achard P, Polymer, **47**, 7636, (2006)
17. Innerlohinger J, Weber HK, Kraft G, *Macromol Symposia,* **244**, 126, (2006).
18. Liebner F, Haimer E, Potthast A, Loidl D, Tschegg S, Neouze M-A, Wendland M, Rosenau T, Cellulosic aerogels as ultra-lightweight materials. Part 2: synthesis and properties, **63**, 3, (2009).
19. Liebner F, Haimer E, Wendland M, Neouze M-A, Schlufter P, Miethe P, Heinze T, Potthast A, Rosenau T, Macromol Biosci **10**, 349, (2010).
20. Aljaberi A, Chatterji A, Shah NH, Sandhu HK, Drug Development and Industrial Pharmacy, **35**, 1066, (2009).
21. Gill RS, Marquez M, Larsen G, Micropor Mesopor Mater, **85**, 129(2005).
22. Goncalves G, Marques PAAP, Trindade T, Pascoal Neto C, Gandini A, J Colloid Interface Sci, **324**, 42, (2008).
23. Tanaka K, Kozuka H, J Sol-Gel Sci Technol, **32**, 73, (2004).